

Concentration-dependent toxicity of iron oxide nanoparticles mediated by increased oxidative stress

Saba Naqvi¹
Mohammad Samim²
MZ Abdin³
Farhan Jalees Ahmed⁴
AN Maitra⁵
CK Prashant⁶
Amit K Dinda⁶

¹Faculty of Engineering and Interdisciplinary Sciences,

²Department of Chemistry,

³Department of Biotechnology, Faculty of Science, ⁴Department of Pharmaceutics, Faculty of Pharmacy, Jamia Hamdard, Hamdard University,

⁵Department of Chemistry, University of Delhi, ⁶Department of Pathology, All India Institute of Medical Sciences, New Delhi, India

Abstract: Iron oxide nanoparticles with unique magnetic properties have a high potential for use in several biomedical, bioengineering and in vivo applications, including tissue repair, magnetic resonance imaging, immunoassay, drug delivery, detoxification of biologic fluids, cell sorting, and hyperthermia. Although various surface modifications are being done for making these nonbiodegradable nanoparticles more biocompatible, their toxic potential is still a major concern. The current in vitro study of the interaction of superparamagnetic iron oxide nanoparticles of mean diameter 30 nm coated with Tween 80 and murine macrophage (J774) cells was undertaken to evaluate the dose- and time-dependent toxic potential, as well as investigate the role of oxidative stress in the toxicity. A 15–30 nm size range of spherical nanoparticles were characterized by transmission electron microscopy and zeta sizer. MTT assay showed >95% viability of cells in lower concentrations (25–200 µg/mL) and up to three hours of exposure, whereas at higher concentrations (300–500 µg/mL) and prolonged (six hours) exposure viability reduced to 55%–65%. Necrosis-apoptosis assay by propidium iodide and Hoechst-33342 staining revealed loss of the majority of the cells by apoptosis. H₂DCFDDA assay to quantify generation of intracellular reactive oxygen species (ROS) indicated that exposure to a higher concentration of nanoparticles resulted in enhanced ROS generation, leading to cell injury and death. The cell membrane injury induced by nanoparticles studied using the lactate dehydrogenase assay, showed both concentration- and time-dependent damage. Thus, this study concluded that use of a low optimum concentration of superparamagnetic iron oxide nanoparticles is important for avoidance of oxidative stress-induced cell injury and death.

Keywords: superparamagnetic iron oxide nanoparticles, cytotoxicity, MTT assay, J774 cell line

Introduction

The exploitation of magnetic nanoparticles for clinical medicine is an important field in the various areas of therapeutics.^{1,2} Due to unique superparamagnetic and other physical properties of iron nanoparticles, they can be fabricated and modified for various nanomedicine applications.^{3,4} These superparamagnetic iron oxide nanoparticles (SPIONs) are of high interest for in vivo applications, including magnetic resonance imaging (MRI) for medical diagnosis, hyperthermia in cancer therapy, magnetofection, tissue repair, drug delivery, and cellular therapy. In cell biology and stem cell research these nanoparticles can be used for cell labeling, cell sorting, separation, and purification procedures.^{5–25} SPIONs can be fabricated with surface modification to make them more biocompatible. They can be conjugated with suitable ligands to target specific receptors of cancer cells for developing targeted delivery systems. Although they appear

Correspondence: Amit K Dinda
(for cellular toxicity studies) All India Institute of Medical Sciences,
New Delhi 110029, India
Tel +91 112 658 8233
Fax +91 112 658 8663
Email amit_dinda@yahoo.com

Mohammad Samim
(for synthesis and characterization of nanoparticles) Department of Chemistry, Jamia Hamdard,
New Delhi 110062, India
Tel +91 11 2605 9688 (ext. 309)
Fax +91 11 2605 9663
Email samim_chem@yahoo.co.in

to be very promising for in vivo application in imaging and drug delivery, it is important to know the safe upper limit of SPIONs for such use.^{26,32-34} Although there are few reports available,²⁶⁻³¹ more elaborate studies are necessary to evaluate concentration-dependent effect of SPIONs on cellular function and toxicity.

Macrophages constitute the central cellular compartment of the reticuloendothelial or mononuclear phagocytic system. They are unique among all other immune cells in that they can enter any tissue and reside there as tissue macrophages, adapting and showing characteristics depending on the tissue they populate. Hence, they are found, eg, as Kupffer cells in the liver, mesangial cells in the kidney, microglial cells in the brain, alveolar macrophages in the lungs, and osteoclasts in bone. Macrophages scavenge for dead cells, as well as any foreign particles, promptly engulfing them. The nature of the material phagocytosed would determine whether the macrophage would become activated or not. Activated macrophages produce inflammatory molecules that signal other cells of the innate and adaptive immune systems about an invasion of the body by some unwanted substance or pathogen that needs to be dealt with. Activated macrophages generate reactive oxygen species (ROS) in a phenomenon called “oxidative burst”, which helps in the killing of ingested microbes.

Nanoparticles delivered in vivo by the systemic route or in a local compartment would undoubtedly be intercepted by the mononuclear phagocytic system, because these are foreign bodies to be phagocytosed.³⁵ In the present study, we wanted to clarify how macrophages react to the presence of SPIONs, ie, whether they get activated or sustain injury from the phagocytosed nanoparticles.

Current in vitro studies have reported the synthesis of Tween 80-coated SPIONs of mean diameter 30 nm. Their interaction with murine macrophage (J774) cells was undertaken to evaluate the dose- and time-dependent toxic potential, as well as to investigate the role of oxidative stress in toxicity.

Materials and methods

Preparation of SPIONs

The SPIONs were prepared in aqueous medium in the following manner. Tween 80 200 μ L was added to 10 mL ferrous sulphate solution 3% (w/v) to form a clear solution. Dissolved oxygen was removed by creating a nitrogen atmosphere. Sodium hydroxide 0.1% (w/v) was then added dropwise under a nitrogen atmosphere and ice-cold temperature, until a blue-green precipitate appeared. The solution containing

the precipitate was stirred for a further two hours to oxidize ferrous to ferric iron partially. The precipitate was then washed four times with aqueous ammonia to wash off excess Tween 80, and the salt was separated by centrifugation at 15,000 rpm for 30 minutes. The resulting brown-colored precipitate was then heated to approximately 60°C for half an hour under vacuum. A blackish-brown powder was obtained and used for further experimentation.

Determination of particle size and shape

The size and morphology of the nanoparticles were determined by transmission electron microscopy (TEM) in the following manner. One drop of the aqueous dispersion of SPIONs followed by one drop of 1% phosphotungstic acid were then put on a formvar-coated copper grid (1% solution of formvar was prepared in spectroscopic grade chloroform) and then air-dried in a vacuum desiccator. The dried grid was examined under a Philips Morgagni 268 electron microscope in the electron microscopy facility at the All India Institute of Medical Sciences, New Delhi, India.

The Malvern Zetasizer 3000HS, which measures particle size based on photon correlation spectroscopy, was used to determine the size distribution of SPIONs at 25°C. Nanoparticles (1 mg) were dispersed in 2 mL double-distilled water by sonication. Size was measured using a 2.42 refractive index and 0.2 absorbance.

Cell culture

The in vitro study was carried out using the murine macrophage cell line, J774 (American Type Culture Collection, Rockville, MD). Confluent macrophages were subcultured and maintained at 37°C in Dulbecco's modified Eagle's medium (Sigma, St. Louis, MO) under a humidified atmosphere (5% CO₂). All media were supplemented with 10% fetal calf serum (Hyclone, Logan, UT), and antibiotic (Sigma) containing 50 U/mL of penicillin and 50 mg/mL of streptomycin and actinomycin.

MTT assay

J774 cells were grown in 96-well plates until subconfluent. Tween 80-coated SPIONs were then added to the cells at defined concentrations (25, 100, 200, 300, 400, and 500 μ g/mL) and incubated for three and six hours. After incubation, the media was discarded and 90 μ L fresh media was added per well to the cells after thorough washing with sterile phosphate-buffered saline. MTT (3-(4,5-dimethylthiazol-2-yl)-2,5-diphenyltetrazolium bromide; Roche Diagnostic,

Mumbai, India) 10 μ L reagent (5 mg/mL stock) was then added per well and the plate was incubated for six hours in an incubator. After incubation, the media was discarded from the wells and dimethyl sulfoxide 100 μ L was added to solubilize the formazan crystals formed. Readings were then taken in a BioRad enzyme-linked immunosorbent assay reader at 490 nm, with subtraction for plate absorbance at 650 nm. Percentage viability of the cells was calculated as the ratio of mean absorbance of triplicate readings with respect to mean absorbance of control wells:

$$\text{Cell viability} = (I_{\text{sample}}/I_{\text{control}}) \times 100.$$

Apoptotic assay

Apoptotic cells were stained with fluorescent dye Hoechst-33342 (Roche) and an apoptotic marker, and counterstained by propidium iodide. Equal number of cells (2×10^4 cells/mL) were seeded and the cells were grown on coverslips in six-well and 12-well plates (TPP, Traisadingen, Switzerland) containing serum-free medium until they were subconfluent at 37°C under 95% CO₂. Cells (2×10^4 cells/mL) were incubated with 25, 200, and 500 μ g/mL SPIONs for three and six hours, respectively. In the control group, nanoparticles were not added to the cells and were incubated for the same time periods. Before terminating the culture, 500 μ L of the culture supernatant was collected from each well for further biochemical assays. The cells were then incubated for 15 minutes with Hoechst-33342 (Roche) at a working dilution of 5 mM and propidium iodide at a final concentration of 50 μ g/mL. Hoechst-33342 is a nuclear stain that labels nuclei blue and can be used as an apoptotic marker.³⁶ Apoptotic cells appear as a strong bright blue color due to the chromatin condensation characteristic of apoptotic cells, while normal healthy cells appear a uniform blue. Hoechst-33342 can enter intact cells without the need for cell membrane permeability, which helps in the identification of early apoptotic cells. Propidium iodide, a dead cell discriminator, was added to discriminate the early apoptotic population from the background of dead cells. Propidium iodide can enter only those cells in which the cell membrane has been damaged, eg, in dead cells or very late apoptotic cells. After staining, cells were washed in phosphate-buffered saline three times for five minutes each, and the coverslips were mounted on slides with 10% glycerol in phosphate-buffered saline. The cells were immediately observed under an upright fluorescent microscope (Eclipse 600; Nikon, Melville, NY) with 488 nm and 350 nm filters, and images were captured using an Olympus DP-71 digital camera (Olympus, Center Valley, PA) mounted on the

microscope. Ten different fields were captured at 40 \times , and subsequently cell counts were taken within the fields to get statistically significant counts for apoptotic cells and viable cells, in each case. Dead cells stained red because of propidium iodide uptake were also counted. The apoptotic cells were quantified as a percentage of the total cell count. Data analysis was performed using Excel (Microsoft Corp., Redmond, WA).

H₂DCFDDA assay

J774 cells (2×10^4 cells/mL) were grown on coverslips until subconfluent. Intracellular ROS was measured using a peroxide-sensitive fluorescent probe, carboxy-2', 7'-dichlorofluorescein diacetate (H₂DCFDDA; Invitrogen, Carlsbad, CA). The cells were loaded with 20 μ M H₂DCFDDA for 60 minutes at 37°C. After loading, the cells were thoroughly washed and fresh media was added. The cells were incubated with the SPIONs at 400 μ g/mL and 500 μ g/mL under standard conditions. After the defined time points, the cells were washed with sterile phosphate-buffered saline and mounted on glycerol phosphate-buffered saline. The cells were observed under a fluorescent microscope (Eclipse 600; Nikon) with a green filter, and the images were captured with a DP-71 digital camera (Olympus). Cells incubated without SPIONs were used as a negative control, and 100 μ M H₂O₂ was used as a positive control.

Lactate dehydrogenase leakage assay

The release of lactate dehydrogenase was monitored by the CytoTox 96 nonradioactive cytotoxicity assay (Promega, Madison, WI). Cells (2×10^4 cells/mL) were placed in 24-well plates and incubated with different concentration of SPIONs (25–500 μ g/mL) for three and six hours. The plates were centrifuged, and aliquots (50 μ L) of cell culture medium were collected from each well and placed in new microtiter plates. Finally, 50 μ L of substrate solution was added to each well and the plates incubated for 30 minutes at room temperature. The absorbance at 490 nm was measured with a microplate reader. Each experiment was done in triplicate. Cytotoxicity is expressed relative to the basal lactate dehydrogenase release by untreated control cells.

Cellular uptake of SPIONs

The SPIONs were incubated with J744 cells at 200 and 500 μ g/mL concentrations for three and six hours. After incubation, the cells are thoroughly washed with cold phosphate-buffered saline (pH 7.5) and fixed with 2% paraformaldehyde

and 1% glutaraldehyde in cacodylate buffer at 4°C for six hours. The cells were osmicated with 1% osmium tetroxide. They were scraped from the culture plate and cell blocks were made in agar. The cell blocks were processed by dehydration, embedded in Epon and polymerized at 60°C. Ultrathin sections were cut from the cell blocks, stained with uranyl acetate and lead citrate, and viewed under an electron microscope (Morgagni 268; Philips, Amsterdam, Netherlands).

Statistical analysis

Statistical analyses were performed using the Student's *t*-test for unpaired data, and *P* values < 0.05 were considered statistically significant. Data are presented as means \pm standard error of the mean.

Results and discussion

The size and shape of SPIONs prepared in aqueous medium were determined by zeta sizer and TEM. The measurements were done by dispersing the SPIONs in double-distilled water using ultrasonic vibration. From dynamic light scattering data shown in Figure 1, the mean diameters of SPIONs made in aqueous medium were found to be around 30 nm, with some polydispersity. The TEM image shown in Figure 2 depicts the spherical shape and confirms the size of the particles to be similar to the zeta size results.

The results of the MTT assay demonstrated that cells exposed to SPIONs of mean size 30 nm for three and six hours resulted in time-dependent as well as concentration-dependent cytotoxicity. At 25 $\mu\text{g}/\text{mL}$ concentration, the viability of cells at three and six hours was 100% and 95%, respectively. With increasing concentration of SPIONs (25, 100, 200, 300, 400, and 500 $\mu\text{g}/\text{mL}$), the percentage viability was decreased from 100% to approximately 75% in three hours. When the cells were incubated with the same concentration of SPIONs for six hours at 25 and 100 $\mu\text{g}/\text{mL}$,

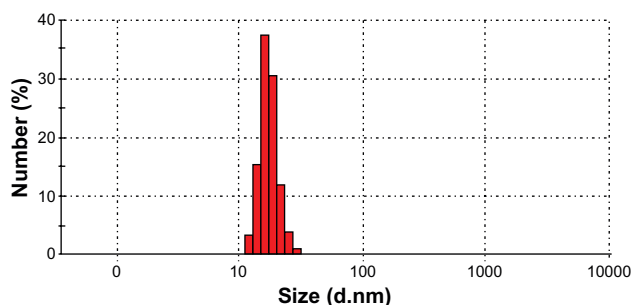


Figure 1 Zeta sizer picture of superparamagnetic iron oxide nanoparticles showing size distribution in aqueous medium.

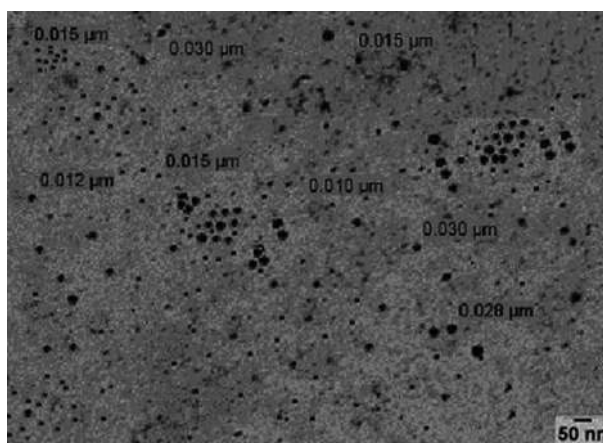


Figure 2 Transmission electron microscopy of superparamagnetic iron oxide nanoparticles.

the cell viability was similar to that at three hours. In contrast, at 200 $\mu\text{g}/\text{mL}$ and higher concentrations, the viability decreased significantly, ranging from 55% to 65% (Figure 3).

We tested the potential for SPION-induced oxidative stress by evaluating intracellular ROS with H_2DCFDA assay. In this methodology, the cell-permeating nonfluorescent compound is converted to fluorescent dichlorofluorescein when the acetate groups are removed by intracellular esterases and intracellular oxidation. Thus, the generation of ROS is directly proportional to the increase of fluorescent intensity. When J774 cells were exposed to 500 $\mu\text{g}/\text{mL}$ SPIONs at two different time points (three and six hours), there was an increase in fluorescence intensity at three hours

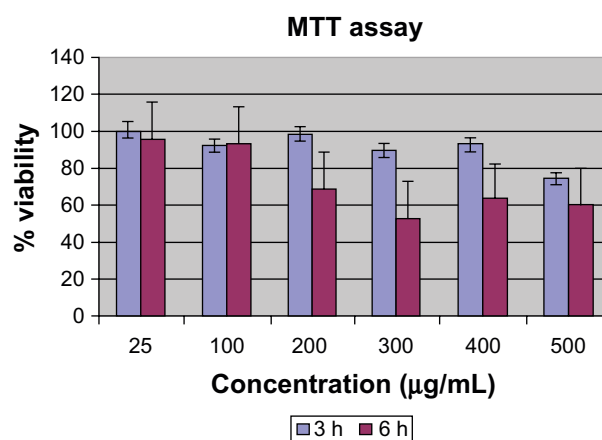


Figure 3 The effects of superparamagnetic iron oxide nanoparticles on cell proliferation and viability of J774 cells as determined by MTT assay. Concentration-dependent cytotoxic effects of nanoparticles evaluated after three and six hours of incubation. Results are represented as means \pm standard error of the mean. **Note:** *Significant difference from control ($P < 0.05$).

in comparison with control cells (Figure 4). After six hours, the intensity increased further. This result indicated that oxidative stress induced by SPIONs was time-dependent. The MTT assay supported this finding because incubation with 500 $\mu\text{g}/\text{mL}$ SPIONs reduced the viability of cells from 75% at three hours to 60% at six hours.

The apoptotic indices of J774 cells following three hours of incubation with 25, 200, and 500 $\mu\text{g}/\text{mL}$ of SPIONs were 1.9 ± 0.6 , 2.5 ± 1.2 , and 26.8 ± 3.5 , respectively. Following six hours of incubation with the same concentration of SPIONs, the indices were 2.1 ± 0.8 , 25.6 ± 2.5 , and 39.4 ± 6.3 . The apoptotic indices of control cells at three and six hours were 1.5 ± 0.6 and 1.6 ± 0.5 (Table 1, Figure 5) This indicated that increased apoptosis of macrophage cells (J774) induced by SPIONs was time- and concentration-dependent, as observed in the MTT assay. Considering the result of the H_2DCFDDA assay for intracellular ROS, it appeared that the increased cellular apoptosis was caused by higher oxidative stress.

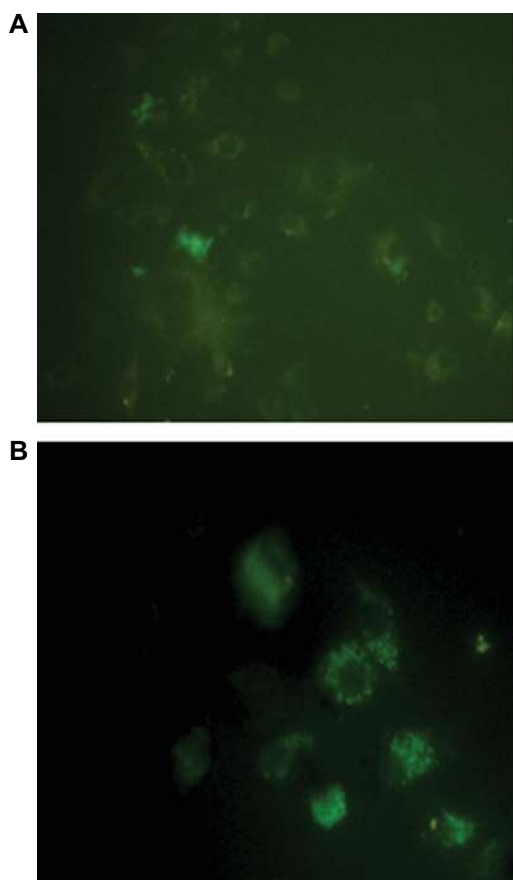


Figure 4 H_2DCFDDA assay for intracellular reactive oxygen species with superparamagnetic iron oxide nanoparticles. **A)** Control and **B)** at concentration of 500 $\mu\text{g}/\text{mL}$.

Table 1 Apoptosis indices of J774 cells following incubation with 25, 200, and 500 $\mu\text{g}/\text{mL}$ of SPIONs for three and six hours

SPION concentration ($\mu\text{g}/\text{mL}$)	Three hours	Six hours
Control	1.5 ± 0.6	1.6 ± 0.5
25	1.9 ± 0.6	2.1 ± 0.8
200	2.5 ± 1.2	$25.6 \pm 2.5^*$
500	26.8 ± 3.5	$39.4 \pm 6.3^*$

Note: $*P < 0.001$.

Abbreviation: SPION, superparamagnetic iron oxide nanoparticle.

Lactate dehydrogenase, a stable cytosolic enzyme in normal cells, can leak into the extracellular fluid only after membrane damage. The exposure of J774 cells to SPIONs for three and six hours showed both concentration- and time-dependent toxicity. These nanoparticles were significantly cytotoxic at higher concentrations when incubated for six hours (Figure 6).

To demonstrate cellular uptake of SPIONs by J774 cells, TEM studies were done following incubation at 200 and 500 $\mu\text{g}/\text{mL}$ concentrations for three and six hours. The SPIONs could be seen in the cytosol as electron-dense par-

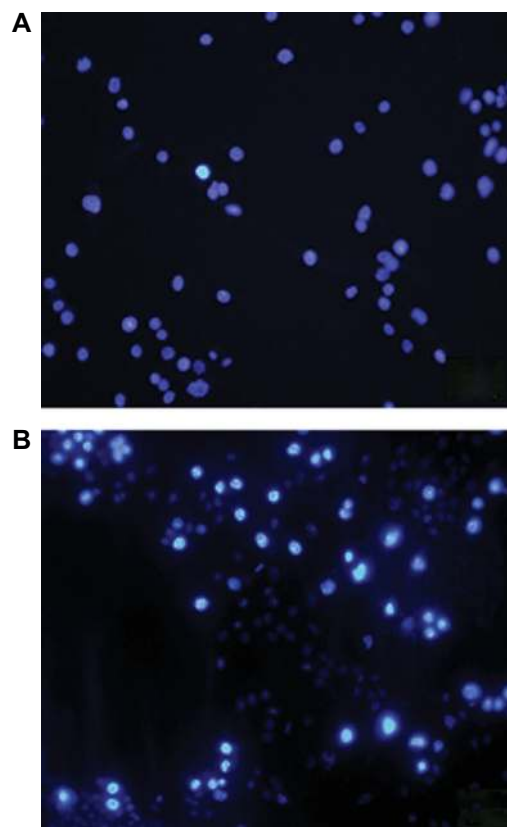


Figure 5 Apoptosis of J774 cells incubated with 500 $\mu\text{g}/\text{mL}$ superparamagnetic iron oxide nanoparticles. **A)** Control and **B)** at six hours. The bright blue nuclei represent apoptosis stained with fluorescent dye Hoechst-33342.

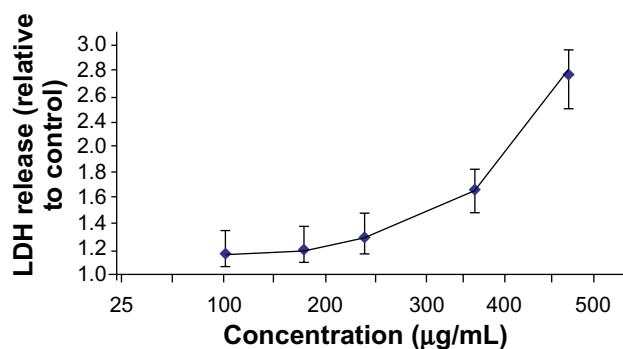


Figure 6 Concentration-dependent membrane damage as determined by lactate dehydrogenase leakage from J774 cell lines (2×10^4 cells/mL) incubated with superparamagnetic iron oxide nanoparticles for six hours.

ticles (Figure 7) at both time points with both concentrations. However, quantification of internalization was not done.

The safety of low SPION concentrations has been demonstrated in earlier studies. To study the efficacy of labeling SPIONs to human neural stem cells, HB1F3 cells were incubated separately for 24 hours with four different types of SPIONs at 25 µg/mL (ie, ferumoxides, MION-47, CLIO-NH₂, and tat-CLIO). The incorporation of SPIONs did not affect cellular proliferation and viability.³⁷ SPIONs coated with dextran (Sinerem[®] and Endorem[®]) and polyvinyl alcohols did not show cytotoxicity or production of inflammatory mediators when cells were exposed at low concentration (iron 11.3 µg/mL).³⁸ The uptake of SPIONs by macrophage cells appeared to be via scavenger receptor class A-mediated endocytosis. In the event of systemic use, these particles would be endocytosed by cells of the reticuloendothelial system.³⁹ There is some evidence that a nanoparticle-induced ROS oxidant stress response might be the major mechanism

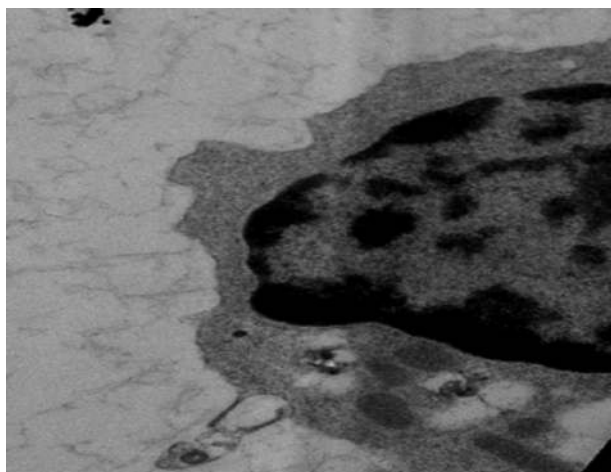


Figure 7 Transmission electron microscopy photograph of J774 cells showing superparamagnetic iron oxide nanoparticles in the cytosol as electron-dense particles following incubation for six hours with 200 µg/mL × 80,000.

for induction of various biologic effects.^{40,41} A recent study demonstrated that exposure to iron nanoparticles induced ROS production in human microvascular endothelial cells.⁴² At low basal levels, ROS appears to be involved in regulating normal cell functions, but at a higher abnormal level might induce cell injury and death.⁴³

Conclusion

SPIONs with a mean size of 30 nm coated with Tween 80 surfactant do not show significant toxicity at concentrations up to 100 µg/mL in murine macrophage (J774) cells with exposure lasting six hours. Toxicity was found to be due to induction of oxidative stress and subsequent apoptosis. An H₂DCFDDA assay to quantify intracellular ROS generation indicated exposure to a higher concentration of nanoparticles, resulting in enhanced ROS generation, leading to cell injury and death. A necrosis-apoptosis assay using propidium iodide and Hoechst-33342 staining revealed that most cell loss was by apoptosis. Therefore, our study concluded that use of low concentrations of SPIONs might be very important for avoiding oxidative stress-induced cell injury and death.

Acknowledgment

The authors are grateful to the Faculty of Engineering and Interdisciplinary Sciences of Jamia Hamdard, Hamdard University, and the Department of Biotechnology, Government of India, for providing financial assistance and support for this research.

Disclosure

The authors have no conflicts of interest to report in this work.

References

1. Lubbe AS, Alexiou C, Bergemann C. Clinical applications of magnetic drug targeting. *J Surg Res*. 2001;95(2):200–206.
2. Polyak B, Friedman G. Magnetic targeting for site-specific drug delivery: Applications and clinical potential. *Expert Opin Drug Deliv*. 2009; 6(1):53–70.
3. Shi J, Gider S, Babcock K, et al. Magnetic clusters in molecular beams, metals, and semiconductors. *Science*. 1996;271:937–941.
4. Sastry M. Moving nanoparticles around: Phase-transfer processes in nanomaterials synthesis. In: Rao CNR, Achim Muller HC, Cheetham AK, editors. *The Chemistry of Nanomaterials*. Weinheim, Germany: Wiley-VCH, Verlag GmbH and Co. KGaA; 2005.
5. Lubbe AS, Bergemann C, Riess H, et al. Clinical experiences with magnetic drug targeting: A phase I study with 4'-epidoxorubicin in 14 patients with advanced solid tumors. *Cancer Res*. 1996;56(20):4686–4693.
6. Strom V, Hultenby K, Gruttner C, et al. A novel and rapid method for quantification of magnetic nanoparticle-cell interactions using a desktop susceptometer. *Nanotechnology*. 2004;15(5):457–466.
7. Rudge S, Peterson C, Vessely, et al. Adsorption and desorption of chemotherapeutic drugs from a magnetically targeted carrier (MTC). *J Control Release*. 2001;74(1–3):335–340.
8. Hood JD, Bednarski M, Frausto R, et al. Tumor regression by targeted gene delivery to the neovasculature. *Science*. 2002;296(5577):2404–2407.

9. Christie RJ, Grainger DW. Design strategies to improve soluble macromolecular delivery constructs. *Adv Drug Deliv Rev.* 2003;55(3): 421–437.
10. Schütt W, Grüttner C, Häfeli U, et al. Applications of magnetic targeting in diagnosis and therapy – possibilities and limitations: A mini-review. *Hybridoma.* 1997;16:109–117.
11. Schütt W, Grüttner C, Teller J, et al. Biocompatible magnetic polymer carriers for in vivo radionuclide delivery. *Artif Organs.* 1999;23(1): 98–103.
12. Shen YF, Tang J, Nie ZH, et al. Preparation and application of magnetic Fe₃O₄ nanoparticles for wastewater purification. *Sep Purif Technol.* 2009;68(3):312–319.
13. Ugelstad J, Stenstad P, Kilaas L, et al. Monodisperse magnetic polymer particles. New biochemical and biomedical applications. *Blood Purif.* 1993;11(6):349–369.
14. Moghimi SM, Hunter ACH, Murray JC. Long-circulating and target-specific nanoparticles: Theory to practice. *Pharmacol Rev.* 2001;53(2): 283–318.
15. Uchegbu IF, Florence AT. Adverse drug events related to dosage forms and delivery systems. *Drug Saf.* 1996;14(1):39–67.
16. Babes L, Denizot B, Tanguy G. Synthesis of iron oxide nanoparticles used as MRI contrast agents: A parametric study. *J Colloid Interface Sci.* 1999;212(2):474–482.
17. Pouliquen D, Le Jeune JJ, Perdrisot R. Iron oxide nanoparticles for use as an MRI contrast agent: Pharmacokinetics and metabolism. *Magn Reson Imaging.* 1991;9(3):275–283.
18. Rinck PA, Myhr G, Smevik O. Oral magnetic particles as an MR contrast medium for the gastrointestinal tract. *Rofo.* 1992;157(6):533–538.
19. Peng XH, Qian X, Mao H, et al. Targeted magnetic iron oxide nanoparticles for tumor imaging and therapy. *Int J Nanomedicine.* 2008;3(3): 311–321.
20. Funovics MA, Kapeller B, Hoeller C, et al. MR imaging of the her2/neu and 9.2.27 tumor antigens using immunospecific contrast agents. *Magn Reson Imaging.* 2004;22(6):843–850.
21. Yang J, Lee CH, Ko HJ, et al. Multifunctional magneto-polymeric nanohybrids for targeted detection and synergistic therapeutic effects on breast cancer. *Angew Chem Int Ed Engl.* 2007;46(46):8836–8839.
22. Alexiou C, Arnold W, Klein RJ, et al. Locoregional cancer treatment with magnetic drug targeting. *Cancer Res.* 2000;60(23):6641–6648.
23. Meng J, Fan J, Galiana G, et al. LHRH-functionalized superparamagnetic iron oxide nanoparticles for breast cancer targeting and contrast enhancement in MRI. *Mater Sci Eng C.* 2009;29(4):1467–1479.
24. Sun C, Lee JSH, Zhang M. Magnetic nanoparticles in MR imaging and drug delivery. *Adv Drug Del Rev.* 2008;60(11):1252–1265.
25. Xu C, Sun S. Monodisperse magnetic nanoparticles for biomedical applications. *Polym Int.* 2007;56(7):821–826.
26. Gupta AK, Curtis ASG. Surface modified superparamagnetic nanoparticles for drug delivery: Interaction studies with human fibroblasts in culture. *J Mater Sci Mater Med.* 2004;15(4):493–496.
27. Lacava ZGM, Azevedo RB, Martins EV, et al. Biological effects of magnetic fluids: Toxicity studies. *J Magn Magn Mater.* 1999;201(1–3): 431–434.
28. Berry CC, Wells S, Charles S, et al. Cell response to dextran-derivatised iron oxide nanoparticles post internalisation. *Biomaterials.* 2004;25(23): 5405–5413.
29. Berry CC, Wells S, Charles S, et al. Dextran and albumin derivatised iron oxide nanoparticles: Influence on fibroblasts in vitro. *Biomaterials.* 2003;24(25):4551–4557.
30. Hilger I, Fruhauf S, Linn S, et al. Cytotoxicity of selected magnetic fluids on human adenocarcinoma cells. *J Magn Magn Mater.* 2003;261(1–2):7–12.
31. Zhang Y, Kohler N, Zhang M. Surface modification of superparamagnetic magnetite nanoparticles and their intracellular uptake. *Biomaterials.* 2002;23(7):1553–1561.
32. Kohler N, Sun C, Wang J, et al. Methotrexate-modified superparamagnetic nanoparticles and their intracellular uptake into human cancer cells. *Langmuir.* 2005;21(19):8858–8864.
33. Sonvico F, Mornet S, Vasseur S, et al. Folate-conjugated iron oxide nanoparticles for solid tumor targeting as potential specific magnetic hyperthermia mediators: Synthesis, physicochemical characterization, and in vitro experiments. *Bioconjug Chem.* 2005;16(5):1181–1188.
34. Zhang Y, Sun C, Kohler N, et al. Self-assembled coatings on individual monodisperse magnetite nanoparticles for efficient intracellular uptake. *Biomed Microdevices.* 2004;6(1):33–40.
35. Mahajan S, Prashant CK, Koul V, Choudhary V, Dinda AK. Receptor specific macrophage targeting by mannose-conjugated gelatin nanoparticles: An in-vitro and in-vivo study. *Curr Nanosci.* 2010;6(4): 413–421.
36. Frenklakh L, Bhat RS, Bhaskaran M, et al. Morphine-induced degradation of the host defense barrier role of intestinal mucosal injury. *Dig Dis Sci.* 2006;51(2):318–325.
37. Song M, Moon WK, Kim Y, Lim D, Song IC, Yoon BW. Labeling efficacy of superparamagnetic iron oxide nanoparticles to human neural stem cells: Comparison of ferumoxides, monocrySTALLINE iron oxide, cross-linked iron oxide (CLIO)-NH₂ and tat-CLIO. *Korean J Radiol.* 2007;8(5):365–371.
38. Cengelli F, Maysinger D, Tschudi-Monnet F, et al. Interaction of functionalized superparamagnetic iron oxide nanoparticles with brain structures. *J Pharmacol Exp Ther.* 2006;318(1):108–116.
39. Raynal I, Prigent P, Peyramaue S, Najid A, Rebutti C, Corot C. Macrophage endocytosis of superparamagnetic iron oxide nanoparticles: Mechanisms and comparison of ferumoxides and ferumoxtran-10. *Invest Radiol.* 2004;39(1):56–63.
40. Nel A, Xia T, Madler L, Li N. Toxic potential of materials at the nano-level. *Science.* 2006;311(5761):622–627.
41. Gwinn MR, Vallyathan V. Nanoparticles: Health effects – pros and cons. *Environ Health Perspect.* 2006;114(12):1818–1825.
42. Apopa PL, Qian Y, Shao R, et al. Iron oxide nanoparticles induce human microvascular endothelial cell permeability through reactive oxygen species production and microtubule remodeling. *Part Fibre Toxicol.* 2009;6:1–14.
43. Lum H, Roebuck KA. Oxidant stress and endothelial cell dysfunction. *Am J Physiol Cell Physiol.* 2001;280(4):C719–C741.